

Using $Z \leq 2$ data to constrain cosmic ray propagation models

Juan Wu*

School of Mathematics and Physics, China University of Geosciences, Wuhan 430074, China

E-mail: wu@cug.edu.cn

Yu Wang

School of Mathematics and Physics, China University of Geosciences, Wuhan 430074, China

E-mail: wangyu45@cug.edu.cn

The boron-to-carbon ratio is usually used to investigate cosmic ray transport processes. However, the results based on the boron-to-carbon ratio remains unclear. In this work, we employ other secondary-to-primary ratios including the deuteron-to-helium 4 ratio, the helium 3-to-helium 4 ratio and the antiproton-to-proton ratio measured by recent experiments to constrain cosmic ray propagation models. Statistical tools are interfaced with the GALPROP package to perform the analysis. Both the force-field approximation and a time-, charge-, and rigidity-dependent solar modulation model are considered to better explore the systematic uncertainties caused by solar effect. The estimated propagation parameters are compared with those derived by using the boron-to-carbon ratio to help us further understand the cosmic ray propagation mechanisms.

*36th International Cosmic Ray Conference -ICRC2019-
July 24th - August 1st, 2019
Madison, WI, U.S.A.*

*Speaker.

1. Introduction

Cosmic ray (CR) physics including their origin, acceleration and propagation are long-standing issues which are still under debate. Recently, thanks to the great improvement on the performances of CR detectors such as PAMELA [1] and AMS02 [2], individual CR elements has been measured with unprecedented accuracies over a wide energy range. Such high quality data enable us to study the CR acceleration and transport behaviours more substantially and reliably.

In previous theoretical studies, the most commonly used secondary-to-primary (S/P) ratio was the boron-to-carbon (B/C) ratio. The diffusion-reacceleration (DR) model was usually preferred which could naturally reproduce the B/C feature around 1 GeV (e.g. see [3, 4, 5]). However, it has been argued that low-mass CR species might suffer different propagation properties with respect to the heavier elements [6]. On the other hand, the DR model favored by the B/C ratio is also disputed by the energetic problem [7]. Considering the possible deficiency by only using the B/C data, an employment of the $Z \leq 2$ secondaries will be useful to help us complement our understanding on CR phenomena. This article aims to use the $Z \leq 2$ CRs and the $Z > 2$ CRs respectively to constrain CR acceleration and propagation models. The derived results will be compared with each other to check whether the light and heavy particles have compatible conclusions.

2. Data Sets

We divide the data sets into two parts. One involves the low-mass elements, i.e. the antiproton-to-proton (\bar{p}/p) ratio, the deuteron-to-helium 4 (${}^2\text{H}/{}^4\text{He}$) ratio, the helium 3-to-helium 4 (${}^3\text{He}/{}^4\text{He}$) ratio together with the proton (p) and helium (He) fluxes. The ${}^2\text{H}/{}^4\text{He}$ and ${}^3\text{He}/{}^4\text{He}$ ratios are available from PAMELA [8]. Other species are measured by both PAMELA [9] and AMS02 [10, 11]. The AMS02 data cover a period of polarity reversal in Heliosphere magnetic field (HMF). In order to facilitate the solar modulation calculation, we only utilize AMS02 data above 20 GeV. Besides, the interstellar proton and helium spectra observed by Voyager-1 are incorporated in our analysis to place robust constraints on solar modulation [12].

The other subset includes the B/C ratio and the carbon (C) flux measured by PAMELA [13] and AMS02 [14, 11]. Still, only data with energies >20 GeV are extracted from AMS02. To complement the lack of data at low energies, the B/C and C data measured by ACE¹ during the same observational time of PAMELA are employed. The Voyager-1 data [12] are also used to test the validity of the solar modulation models. To summarize, all the data used in our analysis are listed in Table 1.

3. Parameter description

After being accelerated at supernova remnant (SNR) shocks, CR particles are released into the interstellar medium (ISM). According to the diffusive shock acceleration theory, the injected density q for a CR species i is expected to follow a rigidity power law. Assuming $f(R, z)$ is the spatial distribution of sources in Galaxy, the general form of the source term is given as:

$$q_i = N_i f(R, z) \rho^{-\nu}, \quad (3.1)$$

¹http://www.srl.caltech.edu/ACE/ASC/level2/lv12DATA_CRIS.html

Subset	Data	Experiment	Energy range	Number of points
$Z \leq 2$	\bar{p}/p	PAMELA	125 MeV \sim 180 GeV	23
		AMS02	20 GeV \sim 450 TeV	26
	$^2\text{H}/^4\text{He}$	PAMELA	100 MeV/n \sim 1.4 GeV/n	24
	$^3\text{He}/^4\text{He}$	PAMELA	100 MeV/n \sim 1.1 GeV/n	21
	p	PAMELA	400 MeV \sim 1.2 TeV	80
		AMS02	20 GeV \sim 1.8 TeV	41
		Voyager-1	3 MeV/n \sim 346 MeV/n	15
	He	PAMELA	100 MeV/n \sim 600 GeV/n	83
		AMS02	20 GeV \sim 1.5 TeV	33
		Voyager-1	3 MeV/n \sim 661 MeV/n	16
$Z > 2$	B/C	PAMELA	440 MeV \sim 130 GeV	18
		AMS02	20 GeV \sim 1 TeV	32
		ACE-CRIS	72 MeV \sim 170 GeV	6
		Voyager-1	5 MeV \sim 117 MeV	9
	C	PAMELA	440 MeV \sim 130 GeV	18
		AMS02	20 GeV \sim 1.5 TeV	33
		ACE-CRIS	68 MeV \sim 195 GeV	7
		Voyager-1	5.4 MeV \sim 137 MeV	12

Table 1: Data sets used in the fitting procedure.

where N_i is the normalization abundance for the CR species i . Different injection indices v_1 and v_2 above and below a reference rigidity ρ_{br} are suggested in our previous work [15]. Moreover, individual species may have different injection spectra. Here we adopt respective v_1 , v_2 and ρ_{br} for p, He and C. All these injection parameters are allowed to vary freely. In GALPROP [16, 17], the source abundance of protons N_p is normalized based on the propagated proton spectrum at 100 GeV and is allowed to vary freely. The normalization abundances of other species are scaled by their source abundances relative to that of protons. To fit the C (or He) data, the C (or He) source abundance relative to proton is set to be free, i.e. X_C (or X_{He}). In this work the production cross-sections of ^2H and ^3He provided in [18] are adopted to give better description of ^2H and ^3He data [19].

During propagation in Galaxy, CR particles scatter mainly on resonant magnetic fluctuations. As expected from the quasi-linear theory, the diffusion coefficient D_{xx} is assumed as:

$$D_{xx} = D_0 \beta^\eta \left(\frac{\rho}{\rho_0} \right)^\delta, \quad (3.2)$$

where D_0 is the normalization of diffusion coefficient at a reference rigidity ρ_0 , $\beta = v/c$ is the particle velocity, η is a low energy dependence factor which could possibly caused by the MHD turbulence dissipation effect [20] and δ is the diffusion slope associated to the spectral index of turbulence spectrum. The free parameters linked to diffusion include D_0 , δ and η .

Diffusion may also happen in momentum space, which results in reacceleration of CR particles. The associated diffusion coefficient in momentum space D_{pp} is correlated to the spatial diffusion coefficient D_{xx} as:

$$D_{pp} = \frac{4v_A^2 p^2}{3\delta(4-\delta^2)(4-\delta)D_{xx}}, \quad (3.3)$$

where v_A is the turbulence velocity in the hydrodynamical plasma, called the *Alfvén velocity*. v_A is the main free parameter related to reacceleration. Other propagation mechanisms like convection via a Galactic wind may also occur. The convection velocity $V_c(z)$ is usually expected to vary linearly with the distance from Galactic plane:

$$V_c(z) = V(0) + \frac{dV}{dz}z, \quad (3.4)$$

in which $V(0)$ is usually set to 0 km/s for the sake of the continuity on convection velocity at Galactic plane. This choice is also suggested in [15]. The parameter dV/dz is allowed to be free.

After entering the Solar system, CRs are modulated by Solar wind. The force-field approximation [21] is a most widely used model for heliospheric modulation. It depends on one free parameter, the Fisk potential Φ . Some studies treated the solar effect in a more reasonable way [22, 23, 24]. In this work, we use both the force-field approximation (referred as FF model) and a physically motivated heliospheric model proposed in [22] (referred as CM model). The CM model takes into account a rigidity-dependent potential Φ , which is expressed as:

$$\Phi(R, t) = \phi_0 \left(\frac{|B_{\text{tot}}|}{4 \text{ nT}} \right) + \phi_1 H(-qA(t)) \left(\frac{|B_{\text{tot}}|}{4 \text{ nT}} \right) \times \left(\frac{1 + (R/R_0)^2}{\beta (R/R_0)^3} \right) \left(\frac{\alpha(t)}{\pi/2} \right)^4, \quad (3.5)$$

where q , R and β are the CR particle's charge, rigidity and velocity, A and $|B_{\text{tot}}|$ are the polarity and magnitude of the HMF measured at Earth, $\alpha(t)$ is the tilt angle of the heliospheric current sheet (HCS), R_0 is a reference rigidity, ϕ_0 and ϕ_1 are two normalization factors. For $qA(t) < 0$, $H(-qA(t))$ is equal to 1. CRs undergo a drift movement along the HCS. For $qA(t) > 0$, $H(-qA(t)) = 0$. CRs travel rather directly from the polar regions of the heliopause to Earth. Here we set R_0 to 0.5 GV [22], and allow ϕ_0 and ϕ_1 to vary freely.

4. Results

Instead of a time-consuming Bayesian analysis, in this work we perform a χ^2 minimization to efficiently discriminate improper models. The systematic uncertainties by using different combinations of data sets can be effectively studied by this method. The minimization library MINUIT [25] is interfaced with GALPROP (version r2766²) for the analysis. The fittings are performed separately by using the $Z \leq 2$ and $Z > 2$ data. For these two cases, we let the nuclear chain start from ^4He and from ^{30}Si respectively. To calculate the p, He and C fluxes, we take into account the contribution from their isotopes. Several benchmark propagation models are investigated in this work: (1) the plain diffusion model with an ad hoc break in the diffusion coefficient (PDbr), (2) the diffusion-reacceleration model (DR), (3) the diffusion-convection model (DC); (4) the diffusion-reacceleration-convection model (DRC). Take into account the solar modulation model used, we add corresponding suffixes "-FF" or "-CM" for all the configurations.

4.1 Fit to the $Z \leq 2$ data

We first test the constraint capability of the \bar{p}/p and p data. A simplest plain diffusion model

²<https://sourceforge.net/projects/galprop/>

without any break in the diffusion coefficient gives a reduced χ^2 equal to 1.09, which means that other mechanisms are not required to describe the data. This infers that only using the \bar{p}/p and p data is not enough for us to discriminate models. As suggested in [15, 18], the secondaries produced by helium nuclei interacting with ISM, as well as the helium flux, are also allowing us to place constraints on acceleration and propagation parameters. Therefore we use all the $Z \leq 2$ data listed in Table 1 to run the analysis.

Parameter	PDbr-FF	DR-FF	PDbr-CM	DR-CM
D_0 ($10^{28} \text{cm}^2 \text{s}^{-1}$)	3.97 ± 0.08	4.45 ± 0.09	4.24 ± 0.08	3.82 ± 0.08
δ_1	-0.32 ± 0.04	0.337 ± 0.008	-0.13 ± 0.04	$0.400 \pm_{0.009}^{0.008}$
δ_2	0.356 ± 0.008	[= δ_1]	0.420 ± 0.009	[= δ_1]
ρ_0 (GV)	$3.86 \pm_{0.11}^{0.16}$	[4]	$6.22 \pm_{0.20}^{0.22}$	[4]
η	1.37 ± 0.12	0.03 ± 0.06	$1.69 \pm_{0.13}^{0.12}$	-0.23 ± 0.07
v_A (km s^{-1})	—	$14.1 \pm_{1.0}^{0.9}$	—	$10.8 \pm_{1.4}^{1.2}$
v_1	$1.43 \pm_{0.05}^{0.04}$	1.709 ± 0.018	$1.548 \pm_{0.024}^{0.023}$	$1.904 \pm_{0.013}^{0.012}$
v_2	2.462 ± 0.008	2.458 ± 0.008	2.394 ± 0.009	$2.404 \pm_{0.008}^{0.009}$
ρ_{br} (GV)	$1.46 \pm_{0.11}^{0.10}$	$2.77 \pm_{0.08}^{0.09}$	$1.70 \pm_{0.23}^{0.06}$	$5.03 \pm_{0.18}^{0.20}$
$v_{1\text{He}}$	1.420 ± 0.019	1.440 ± 0.018	$1.453 \pm_{0.022}^{0.021}$	$1.529 \pm_{0.020}^{0.019}$
$v_{2\text{He}}$	2.392 ± 0.008	2.402 ± 0.007	2.319 ± 0.009	2.321 ± 0.007
$\rho_{br\text{He}}$ (GV)	2.42 ± 0.05	$2.362 \pm_{0.015}^{0.040}$	$2.22 \pm_{0.06}^{0.07}$	$2.03 \pm_{0.08}^{0.07}$
N_p ($10^{-9} \text{cm}^{-2} \text{sr}^{-1} \text{s}^{-1} \text{MeV}^{-1}$)	4.331 ± 0.011	4.326 ± 0.011	4.334 ± 0.011	4.331 ± 0.011
X_{He}	0.020 ± 0.004	$0.106 \pm_{0.008}^{0.009}$	$0.037 \pm_{0.010}^{0.004}$	$0.59 \pm_{0.07}^{0.10}$
ϕ_0 or Φ (GV)	$0.432 \pm_{0.007}^{0.006}$	0.458 ± 0.006	$0.234 \pm_{0.009}^{0.010}$	0.260 ± 0.009
ϕ_1			8.40 ± 0.06	7.47 ± 0.06
$\chi^2/\text{d.o.f}$	1.97	2.30	1.21	1.66

Table 2: The best-fit parameters for PDbr-FF, DR-FF, PDbr-CM and DR-CM models constrained by the $Z \leq 2$ data. The fixed parameters appear in square brackets.

It is found that the convection velocity gradient dV/dz is converged at 0 for all the DC models. For the DRC models, only a weak dV/dz close to 0 is allowed. For those models without convection, the results are shown in Table 2. By incorporating the FF approximation, the best-fit values of the diffusion slope δ_2 are around 0.33~0.36. However, by using the CM model, the estimated slopes are around 0.39~0.43. A variance on δ_2 achieves 18% ~ 20% when we adopt different solar modulation models. But all the models presented in Table 2 agree well with the high energy \bar{p}/p data, as shown in Fig 1. To fit the high-energy proton data, parameters $\delta_2 + v_2$ and N_p remain consistent for all the models, which are about 2.8 and $4.33 \times 10^{-9} \text{cm}^{-2} \text{sr}^{-1}$ respectively. Compared with the proton injection index v_2 , the He injection index $v_{2\text{He}}$ is about 0.5~0.8 harder.

For the low energy CR behaviors, the best-fit parameters are model-dependent. The low energy factor η is much smaller when a reacceleration process is considered. The best-fit values of v_A for the DR-FF and DR-CM models are equal to $14.1 \pm 1.0 \text{km s}^{-1}$ and $10.8 \pm_{1.4}^{1.2} \text{km s}^{-1}$ respectively. Only a moderate reacceleration is needed to explain the low-mass S/P ratios. The shift of the diffusion slope $\delta_2 - \delta_1$ at a few GeV is about 0.5~0.7 for the PDbr models. By assuming different propagation mechanisms, the low energy proton injection indices also show a clear distinction for the DR models and the PDbr models. As we can see from Fig 1, both the PDbr-FF and DR-FF models present prominent estrangements with the PAMELA helium data at sub-GeV range. These discrepancies are highly reduced under the CM scenario. This explains why the χ^2 values are much smaller by employing the CM model. The FF and CM scenarios, which predict significantly

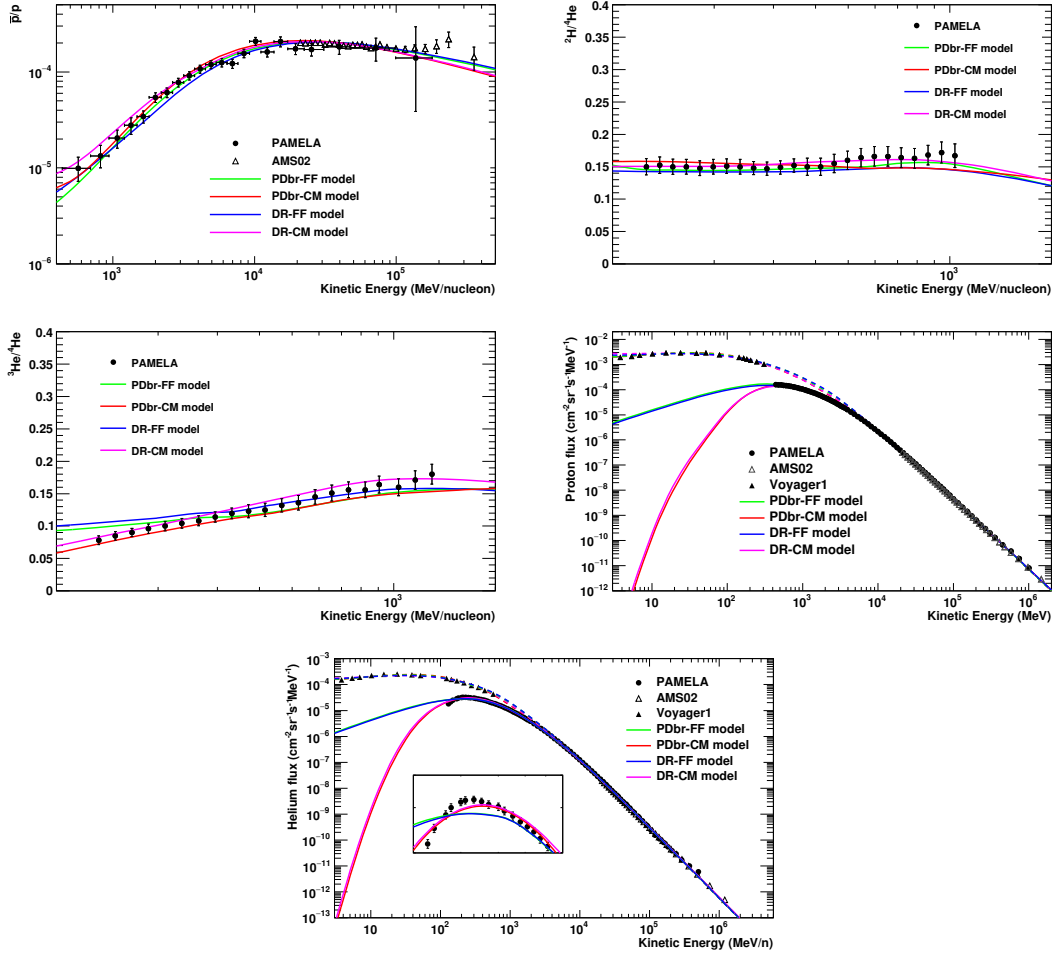


Figure 1: The \bar{p}/p , ${}^2\text{H}/{}^4\text{He}$, ${}^3\text{He}/{}^4\text{He}$ ratios, and the p, He fluxes for the PDbr-FF, DR-FF, PDbr-CM and DR-CM models as listed in Table 2. The solid (dashed) lines represent the modulated (unmodulated) fluxes and ratios.

different modulated primary fluxes at energies below 100 MeV, may be clarified by future low energy data. Nevertheless, current PAMELA helium data from 100 MeV to 400 MeV show a preference for the CM solar modulation.

4.2 Fit to the B/C + C data

Based on the best-fit parameters evaluated from the $Z \leq 2$ data, the theoretical predictions for the B/C ratio and the C flux are presented in Fig 2. All the models show remarkable coincidences with the high energy B/C data. However, for the models under the CM scenario, prominent conflicts with ACE B/C data appear. For the PDbr-CM and DR-CM models, the theoretical modulated B/C ratios show an increasing trend with decreasing energy below 200 MeV. This feature is caused by the dramatically decreased modulated C spectra at the same energy range, which is also conflicting with the C flux measured by ACE.

Despite these discrepancies between the CM model and the ACE data, all the predictions attenuate the bump around 1 GeV exhibited by the B/C data. To better understand the influence of the parameters on B/C ratio, we perform a χ^2 analysis on the B/C and C data. Considering the

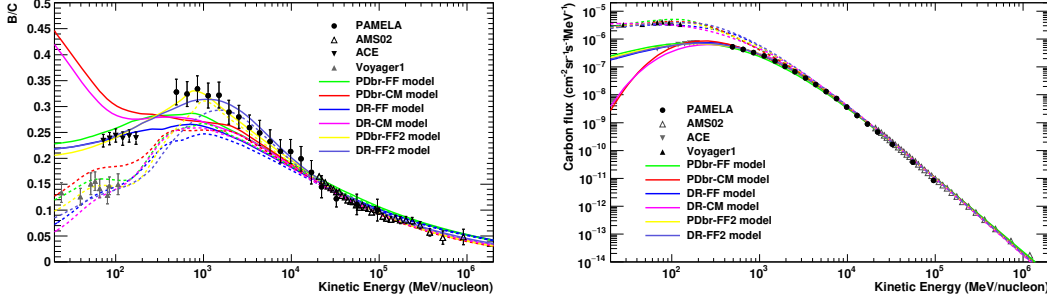


Figure 2: The B/C ratio and the C flux for the PDbr-FF, DR-FF, PDbr-CM, DR-CM, PDbr-FF2 and DR-FF2 models as listed in Table 2 and Table 3. The solid (dashed) lines represent the modulated (unmodulated) fluxes and ratios.

Parameter	PDbr-FF2	DR-FF2
D_0 ($10^{28} \text{cm}^2 \text{s}^{-1}$)	$4.1 \pm_{0.4}^{0.5}$	$2.79 \pm_{0.16}^{0.18}$
δ_1	-1.6 ± 0.4	$0.383 \pm_{0.015}^{0.014}$
δ_2	0.422 ± 0.013	[= δ_1]
ρ_0 (GV)	$3.77 \pm_{0.13}^{0.15}$	[4]
η	$2.7 \pm_{0.6}^{0.7}$	0.42 ± 0.14
v_A (km s^{-1})	—	20.6 ± 0.9
v_{1C}	$0.38 \pm_{0.14}^{0.13}$	0.62 ± 0.15
v_{2C}	2.327 ± 0.013	2.400 ± 0.011
ρ_{br} (GV)	$1.25 \pm_{0.05}^{0.06}$	$1.46 \pm_{0.08}^{0.10}$
X_C (10^{-3})	2.6 ± 0.4	$14.8 \pm_{2.4}^{2.2}$
Φ (GV)	0.440 ± 0.014	0.518 ± 0.014
$\chi^2/\text{d.o.f}$	1.15	1.09

Table 3: The best-fit parameters for PDbr-FF2 and DR-FF2 models constrained by the B/C and C data. The fixed parameters appear in square brackets.

incompetence of the CM model in describing the ACE data, only the FF approximation is used. It is found that the convection mechanism is also disfavored by the heavy nuclei. The best-fit parameters for the models without convection are listed in Table 3. We add a suffix "-FF2" for each model to distinguish with the cases given in Table 2. The values of the diffusion spectral index δ_2 are constrained around 0.4 for the PDbr-FF2 and DR-FF2 models. These two models yield reasonable χ^2 values close to 1. The satisfactory fit can be seen from Fig 2. Compared with the results from the PDbr-FF and DR-FF models, a much larger diffusion slope variation $\delta_2 - \delta_1 \sim 2.0$ or a stronger *Alfvén velocity* v_A is required to reconcile the B/C bump around 1 GeV. Even ignoring the disagreement between the FF models with the low energy helium data, the results extracted from different data subsets still infer distinct low energy CR phenomena.

5. Conclusion

In this work, we use the $Z \leq 2$ elements and the $Z > 2$ nuclei separately to study the acceleration and propagation models. At high energies, the values of diffusion slope δ_2 are estimated between $0.33 \sim 0.43$ for all the models. Though an uncertainty on δ_2 achieving 20% can be led by using different data subsets or by employing different solar modulation assumptions, all these propagation models can fit high energy S/P ratios well. Nevertheless, a Kolmogorov-type turbulence is

preferred rather than a Kraichnan-type turbulence. At low energies, our understanding on CR behaviors is controversial. An agreement is that the convection mechanism is not preferred by all the data. By introducing a reacceleration process or by adopting a break in diffusion coefficient can reproduce either the $Z \leq 2$ particles or the $Z > 2$ nuclei. But a dramatic change on the diffusion slope at a few GeV or a stronger reacceleration process is required by the B/C data. Moreover, a simple force-field approximation can reproduce the B/C and C data well, but it displays inconsistencies with the low energy helium data measured by PAMELA. A rigidity-dependent CM model agrees better with the helium flux, but it is disapproved by the ACE data. These conflictions may be caused by two reasons. One is that we need to improve our theoretical knowledge on the low energy CR physics. The other is that the possible systematic uncertainties on data sets may bias our results. We expect that more accurate data at MeV range may help us clarify this situation.

References

- [1] P. Picozza et al. (PAMELA Collaboration), *Astropart. Phys.* 27, 296 (2007).
- [2] M. Aguilar et al. (AMS Collaboration), *Phys. Rev. Lett.* 110, 141102 (2013).
- [3] R. Trotta et al., *Astrophys. J.* 729, 106 (2011).
- [4] Jia-Shu Niu and Tianjun Li, *Phys. Rev. D* 97, 023015 (2018).
- [5] Qiang Yuan, *Sci.China Phys.Mech.Astron.* 62, 49511 (2019).
- [6] G. Jóhannesson et al., *Astrophys. J.* 824, 16 (2016).
- [7] L. O. Drury and A. W. Strong, *Astron. Astrophys.* 597, A117 (2017).
- [8] O. Adriani et al. (PAMELA Collaboration), *Astrophys. J.* 818, 68 (2016).
- [9] O. Adriani et al. (PAMELA Collaboration), *Science* 332, 69 (2011).
- [10] M. Aguilar et al. (AMS Collaboration), *Phys. Rev. Lett.* 114, 171103 (2015).
- [11] M. Aguilar et al. (AMS Collaboration), *Phys. Rev. Lett.* 119, 251101 (2017).
- [12] A. C. Cummings et al., *Astrophys. J.* 831, 18 (2016).
- [13] O. Adriani et al. (PAMELA Collaboration), *Astrophys. J.* 791, 93 (2014).
- [14] M. Aguilar et al. (AMS Collaboration), *Phys. Rev. Lett.* 117, 231102 (2016).
- [15] Juan Wu and Huan Chen, *Phys. Lett. B* 789, 292 (2019).
- [16] I. V. Moskalenko and A. W. Strong, *Astrophys. J.* 493, 694 (1998).
- [17] A. W. Strong and I. V. Moskalenko, *Astrophys. J.* 509, 212 (1998).
- [18] B. Coste et al., *Astron. Astrophys.* 539, A88 (2012).
- [19] N. Picot-Clémente et al., *Proceedings of the 34th International Cosmic Ray Conference* 555 (2015).
- [20] V. S. Ptuskin et al., *Astrophys. J.* 642, 902 (2006).
- [21] L. J. Gleeson and W.I. Axford, *Astrophys. J.* 154, 1011 (1968).
- [22] I. Cholis, D. Hooper, and T. Linden, *Phys. Rev. D* 93, 043016 (2016).
- [23] C. Corti et al., *Astrophys. J.* 829, 8 (2016).
- [24] M. J. Boschini et al., *Astrophys. J.* 840, 115 (2017).
- [25] F. James and M. Roos, *Computer Physics Communications* 10, 343 (1975).